FLEXIBILITY ANALYSIS OF CAM MECHANISM

M. M. Tayeb and A. S. Sliman

Mechanical and Industrial Engineering Department,
Al-Fateh University, P.O. Box 13276, Tripoli, Libya

الملخص

عند دوران عمود الحدبات بسرعة عالية في محركات السيارات، فإن إستجابة صمامات دخول الهواء وخروج غازات العادم تكون مختلفة عن أوامرالحدبة. الفروقات في الإستجابة عن القيم المطلوبة تسبب العديد من المشاكل في تركيبة الحدبات مثل الإهتزازات والضوضاء. هذه الإختلافات بين المداخل والمخارج هي في الأساس ناتجة عن المرونة في المنظومة التي صممت لتكون صلبة. يتركز هذا البحث حول دراسة تأثير المرونة على إستجابة آلية حدبة محرك السيارة. تم نمذجة بنية الحدبة من عوارض مرنة تحتوي كتل مركزة. وتتكون من عقدتين وعدد 6 درجات حرية (ثلاثة طولية وثلاثة إلتوائية عند كل عقدة). وأستخدامت طريقة العناصر المتناهية في الصغرلإستنتاج المعادلات العامة للحركة بإستخدام طريقة "جاليركن". وتم إستخدام ثلاثة نماذج ذات 4 و 8 و 10 عناصر بها 21 و 25 و 47 درجة حرية وحلها عددياً بإستخدام طريقة " نيومارك" بالتكامل المباشر. ودراسة ثلاثة حالات لحركة الحدبة وهي الحركة التوافقية البسيطة (SHM) وقطع مكافئ (Parabolic) ودويري (Cycloidal). عند مقارنة النتائج المتحصل عليها مع النتائج بإستخدام نموذج صلب تبين أن الفروقات بين إستجابة المنظومة المرنة والمنظومة الصلبة حساس لعدد درجات حرية النموذج. كما يستخلص من هذا البحث أنه لا يمكن إهمال تأثير المرونة على كل من عمود الحدبات وتوابع الحدبات أثناء السرعات العالية. يوصى بإستكمال البحث لدراسة تأثير المرونة والتخميد والإحتكاك في الكراسي على إستجابة الحدبات.

ABSTRACT

In automobile engines, when the cam structure is running at high speed, the response of the inlet air valves and outlet gas valves will be different from the cam input command. The deviation of the system response from the desired values causes various problems in the cam structure such as vibrations and noise which can cause low cam system performance. These differences in action between input and output are basically due to the elasticity of the system which is designed as rigid. This work focuses on the effect of the elasticity on the responses of car engine cam mechanism. The cam structure was modeled as a flexible beam with concentrated mass. The proposed beam elements used in the model have two nodes and six degrees of freedom (DOF), with

three translations and three rotations at each node. The finite element method was used to derive the global equations of motion using Galerkin method. Three models of 4, 8 and 10 elements consisting of 21, 25 and 47 DOF respectively were used as case studies. The derived global equations were solved numerically using Newmark direct integration method. Three different cases of cam motion were studied; simple harmonic, parabolic, and cycloidal were considered as the input signals to the system. The responses from these cases were compared with rigid system analysis. It was concluded that the effect the elasticity of both cam shaft and follower train system at high speed cannot be neglected. It also can be concluded that the flexible system response deviation from rigid system response is sensitive to the DOF of the model. In general, all models responses show higher deviation from the rigid system at cam angle that produces wide open or complete closure of the valve. It is recommended that investigations should be extended to cover the effects of elasticity, friction and damping of bearings on cam system responses.

KEYWORDS: Cam Mechanism; Dynamics; Flexibility; Galerkin Method; Finite Element.

INTRODUCTION

In the case of a cam mechanism running at relatively slowly speed, the response of the valve mass will be the same as the values calculated on the basis of the static cam command. As the operational speed of cam mechanism increases, the deviation of the system response form the desired values are increased. Various problems can arise in the mechanism such as vibrations and noise which can cause low cam performance. These differences in action between the cam and valve are basically due to elasticity in the system elements such as follower train and cam shaft. This means that system components act as springs of various stiffnesses. In addition to this elasticity in the system, the clearances and wear can cause these differences. In modeling of an automotive valve-gear system, the flexibility of follower train of the cam mechanism only was considered [1]. The effect of wind-up of cam shaft on the input tongue of the system was investigated [2]. The effect of cam profile errors and system flexibility on cam mechanism using a more complicated model was presented [3]. This work was continued by [4] in which the dynamic performance of high speed semi-rigid follower cam system and its effects on cam profile errors were studied. Vibration analysis of flexible cam mechanism using variational approach was presented [5].

FLEXIBLE CAM MECHANISM MODEL

In this work, the cam mechanism as presented in Figure (1) was modeled as a flexible beam while the cam was considered as a rigid mass at the cam position. The follower train was modeled as a flexible beam with concentrated masses. These concentrated masses were the equivalent masses of the tappet, retaining spring, rocker arm and valve, while the push rod was considered as flexible beam elements.

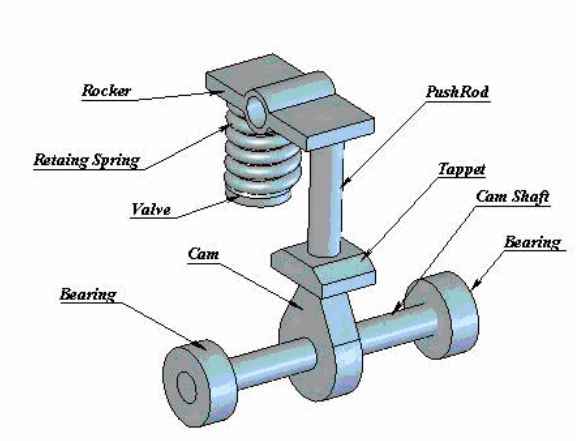

Figure 1: Automotive cam-follower model.

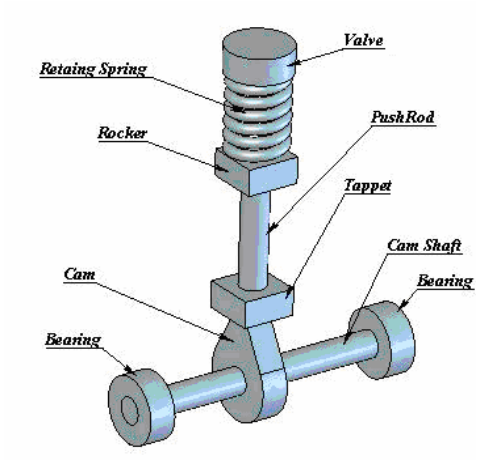

Figure 2: Flexible model .

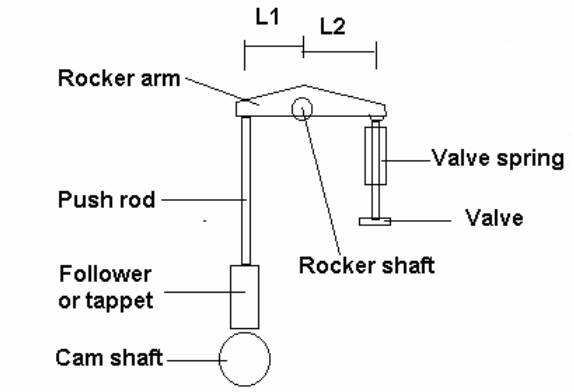

Figure 3: General arrangement of valve gear in an engine.

Figure (2) represents the flexible model of the cam mechanism. The following equations represent the masses and springs equivalent for the flexible model as shown in Figure (3):

$$M_{eq(\,roc\,ker+valve\ Side\,)} = M_{Valve\ Side}\left[\frac{L_2}{L_1}\right]^2 + \left[\frac{I_{roc\,ker}}{L_1^2}\right] \tag{1}$$

$$K_{eq} = \left(\frac{L_2}{L_1}\right) K_{Valve\,spring} \tag{2}$$

GOVERNING DIFFERENTIAL EQUATIONS

The differential equations governing dynamic beam element are presented in the transverses X-Y, X-Z planes, axial and torsional directions. The beam cross-sectional properties are assumed constant along the beam axis. The equations of equilibrium of infinitesimal segments in Figure (4) and Figure (5) are given by:

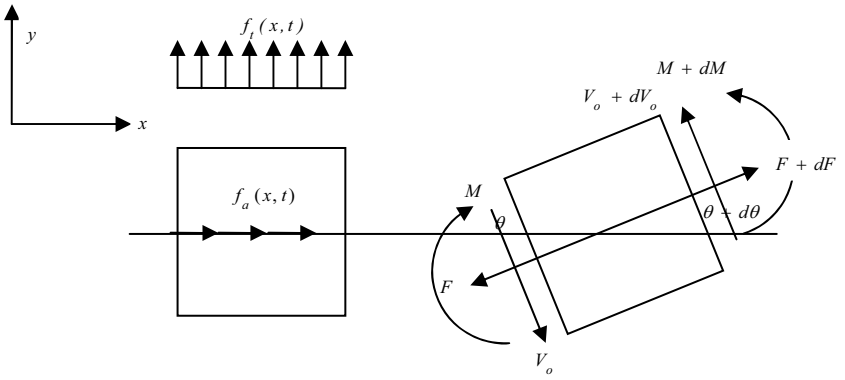

Figure 4: An infinitesimal segment of the beam x-section.

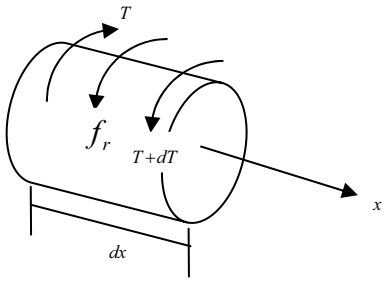

Figure 5: Tongue acting on beam element of length *dx*.

- For axial vibration

$$\rho A \frac{\partial^2 u}{\partial t^2} - \frac{\partial}{\partial x}\left(AE \frac{\partial u}{\partial x} \right) + \frac{\partial}{\partial x}\left(AG \left(\frac{\partial v}{\partial x} \right)^2 \right) - f_a(x,t) = 0 \tag{3}$$

- *For* transverse vibration

$$\rho A \frac{\partial^2 v}{\partial t^2} + \frac{\partial^2}{\partial x^2}(E I \frac{\partial^2 v}{\partial x^2}) - \rho I \frac{\partial^4 v}{\partial t^2 \partial x^2} - \frac{\partial}{\partial x}(AE \frac{\partial u}{\partial x} \frac{\partial v}{\partial x}) - f_t(x,t) = 0 \tag{4}$$

- For torsional vibration

$$\rho J \frac{\partial^2 \theta_x}{\partial t^2} - \frac{d}{dx}\left(GJ \frac{\partial \theta_x}{\partial x} \right) = f_r(x,t) \tag{5}$$

The governing equations will be solved using the boundary conditions. In this work, the problem will be solved numerically using Finite Element Method (FEM).

BEAM ELEMENT

The derivation these elements can be used for the analysis beam element. A beam element is a straight bar of uniform cross section which is capable of resisting axial forces, bending moments about the tow principal axes in the plane of its cross section and twisting moment about its controidal axis. The corresponding displacement degrees of freedom are shown in Figure (6). It can be seen that the stiffness and inertia matrices of a beam element will be of order 12x12.

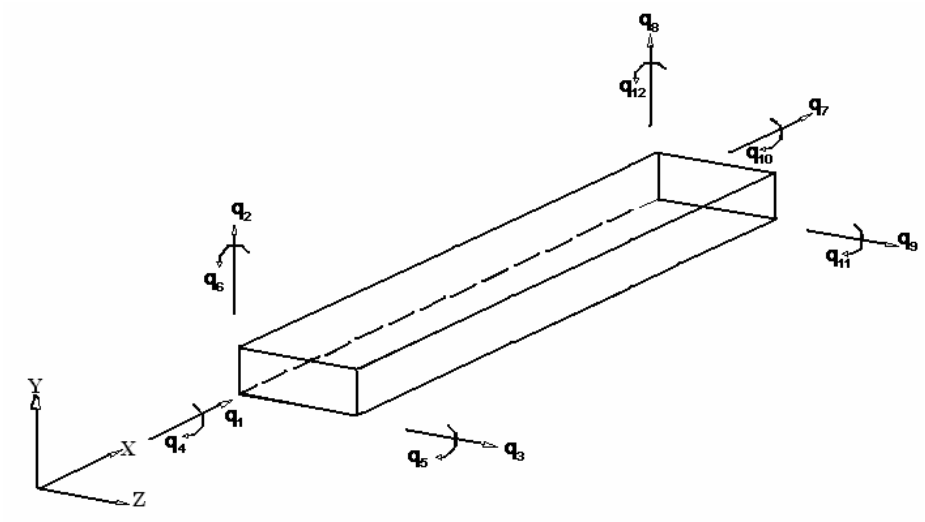

Figure 6: Beam element with 12 degrees of freedom.

The local xyz coordinate system was chosen to coincide with the principle axes of the cross section with x-axis which represents the centroidal axis of the beam element. Thus the displacements can be separated into four groups each of which can be considered independently of others. The stiffness and Inertia matrices corresponding to different independent sets of displacements were considered, and then the total stiffness matrix of the elements was obtained by superposition.

FINITE ELEMENT MODEL

In this section, the matrix equations of the model in a discrete form were obtained using a Finite Element Approach. In this study, the Weighted Residual Approach known as *Galerkin Method* will be used. The governing differential equations for axial motion and associated boundary conditions and initial conditions are presented as follows:

$$\rho A \frac{\partial^2 u}{\partial t^2} - \frac{\partial}{\partial x}\left(AE \frac{\partial u}{\partial x} \right) + \frac{\partial}{\partial x}\left(AG\left(\frac{\partial v}{\partial x} \right)^2 \right) - f_a(x,t) = 0 \tag{6}$$

Two possible boundary conditions are:

- Essential BC's: $u = u_o$
- Natural BC's: $AE \frac{\partial u}{\partial x} = F$, $AG \frac{\partial v}{\partial x} = V_o$ and $AG\left(\frac{\partial v}{\partial x} \right)^2 = \frac{V_o^2}{AG}$

THE GALERKIN RESIDUAL EQUATION

The first Step of the Galerkin method is by minimizing the weighted Residual R:

$$R = \rho A \frac{\partial^2 u}{\partial t^2} - \frac{\partial}{\partial x}\left(AE \frac{\partial u}{\partial x} \right) + \frac{\partial}{\partial x}\left(AG\left(\frac{\partial v}{\partial x} \right)^2 \right) - f_a(x,t) \tag{7}$$

Let the integral of weighted residual equal to zero as :

$$\int_s N_i(x).R.dx = 0 \tag{8}$$

$$\int_{x1}^{x2} \rho^{e} A^{e} \frac{\partial^2 u^{e}}{\partial t^2} N_i^{e} dx - \int_{x1}^{x2} \frac{\partial}{\partial x}\left(A^{e} E^{e} \frac{\partial u^{e}}{\partial x} \right) N_i^{e} dx + \int_{x1}^{x2} \frac{\partial}{\partial x}\left(A^{e} G^{e} \left(\frac{\partial v^{e}}{\partial x} \right)^2 \right) N_i^{e} dx - \int_{x1}^{x2} f_a^{e}(x,t) N_i^{e} dx = 0 \quad (9)$$

Integrate the second and the third terms of Equation (9) by parts, using the basic relation:

$$\int_s \frac{\partial f}{\partial x} g dx = g.f - \int_s \frac{\partial g}{\partial x} f dx \quad (10)$$

Let the second and the third terms in the Equation 9 be in the form:

$$\int_{x1}^{x2} \frac{\partial}{\partial x}\left(A^{e} E^{e} \frac{\partial u^{e}}{\partial x} \right) N_i^{e} dx = \left[\left(A^{e} E^{e} \frac{\partial u^{e}}{\partial x} \right) N_i^{e} \right]_{x1}^{x2} - \int_{x1}^{x2} \left(A^{e} E^{e} \frac{\partial u^{e}}{\partial x} \right) \frac{\partial N_i^{e}}{\partial x} dx \quad (11)$$

$$\int_{x1}^{x2} \frac{\partial}{\partial x}\left(A^{e} G^{e} \left(\frac{\partial v^{e}}{\partial x} \right)^2 \right) N_i^{e} dx = \left[A^{e} G^{e} \left(\frac{\partial v^{e}}{\partial x} \right)^2 N_i^{e} \right]_{x1}^{x2} - \int_{x1}^{x2} A^{e} G^{e} \left(\frac{\partial v^{e}}{\partial x} \right)^2 \frac{\partial N_i^{e}}{\partial x} dx \quad (12)$$

Substituted Equation (11) and Equation (12) into Equation (9) we get:

$$\int_{x1}^{x2} \rho^{e} A^{e} \frac{\partial^2 u^{e}}{\partial t^2} N_i^{e} dx + \int_{x1}^{x2} \left(A^{e} E^{e} \frac{\partial u^{e}}{\partial x} \right) \frac{\partial N_i^{e}}{\partial x} dx - \int_{x1}^{x2} A^{e} G^{e} \left(\frac{\partial v^{e}}{\partial x} \right)^2 \frac{\partial N_i^{e}}{\partial x} dx = \int_{x1}^{x2} f_a^{e}(x,t) N_i^{e} dx + \left[\left(A^{e} E^{e} \frac{\partial u^{e}}{\partial x} \right) N_i^{e} \right]_{x1}^{x2} - \left[A^{e} G^{e} \left(\frac{\partial v^{e}}{\partial x} \right)^2 N_i^{e} \right]_{x1}^{x2} \quad (13)$$

`

Assume a linear interpolation for the field variables $u^{e}(x,t)$; $v^{e}(x,t)$, which can be written as:

$$u^{e}(x,t) = \sum_{j=1}^{2} q_j^{e}(t).N_j^{e}(x) \quad (14)$$

$$v^{e}(x,t) = \sum_{k=1}^{2} q_k^{e}(t).N_k^{e}(x) \quad (15)$$

Substituting the first derivative of Equation (14) and (15) with respect to x into Equation (13), and the first second derivative with respect to t into Equation (13):

$$\left[\int_{x1}^{x2} \rho^{e} A^{e} N_i^{e} N_j^{e} dx \right] \ddot{q}_j + \left[\int_{x1}^{x2} A^{e} E^{e} \frac{\partial N_i^{e}}{\partial x} \frac{\partial N_j^{e}}{\partial x} \right] q_j - \left[\int_{x1}^{x2} A^{e} G^{e} \left| \frac{\partial N_k^{e}}{\partial x} \right| \left(\frac{\partial N_k^{e}}{\partial x} \right) \frac{\partial N_i^{e}}{\partial x} q_k \right] q_k$$
$$= \int_{x1}^{x2} f_a^{e}(x,t) N_i^{e} dx + \left[\left(A^{e} E^{e} \frac{\partial^2 u^{e}}{\partial x^2} \right) N_i^{e} \right]_{x1}^{x2} - \left[A^{e} G^{e} \left(\frac{\partial v^{e}}{\partial x} \right)^2 N_i^{e} \right]_{x1}^{x2} \quad (16)$$

The matrix equation of motion for a nonlinearly undamped beam element is expressed as follows:

$$M_j\ddot{q} + (K_j + K_K)q = P \tag{17}$$

$$\overset{e}{M}_j = \int_{x1}^{x2} \overset{e}{\rho}\overset{e}{A}\overset{e}{N}_j\overset{e}{N}_i\,dx \;;\quad K_j = \int_{x1}^{x2} \overset{e}{A}\overset{e}{E}\frac{\partial \overset{e}{N}_j}{\partial x}\frac{\partial \overset{e}{N}_i}{\partial x}dx \;;\quad \overset{e}{K}_k = \left[\int_{x1}^{x2} \overset{e}{-A}\overset{e}{G}\left|\frac{\partial \overset{e}{N}_k}{\partial x}\right|\left(\frac{\partial \overset{e}{N}_k}{\partial x}\right)\frac{\partial \overset{e}{N}_i}{\partial x}\right] q_k;$$

$$\overset{e}{P} = \int_{x1}^{x2} \overset{e}{f}_a(x,t)\overset{e}{N}_i\,dx + \left[\left(\overset{e}{A}\overset{e}{E}\frac{\partial \overset{e}{u}}{\partial x}\right)\overset{e}{N}_i\right]_{x1}^{x2} - \left[\overset{e}{A}\overset{e}{G}\left(\frac{\partial \overset{e}{v}}{\partial x}\right)^2 \overset{e}{N}_i\right]_{x1}^{x2}$$

The choosing polynomial and its partial derivatives up to one order less than highest order derivative governing differential equation must be continuous at element boundaries or interfaces. It can be seen from Equation (6) that the highest order derivative is two. Then selected order for polynomial is first order:

$$\overset{e}{N}_j(x) = \overset{e}{N}_k(x) = \overset{e}{N}(x) = a_1 + a_2 x \tag{18}$$

To obtain the two unknowns (b_i, i=1, 2), the condition of the nodal waiting values N_1 and N_2 should be defined.

$$N_1 = \begin{cases} 1\ at\ node\ number\ 1 \\ 0\ elsewhere \end{cases} \qquad N_2 = \begin{cases} 1\ \text{at node number}\ 2 \\ 0\ \text{elsewhere} \end{cases}$$

Substituting back into Equation (18), where $x_1 = 0$ and $x_2 = L$. The results become:

$$\overset{e}{N}_1 = 1 - x/L \quad \text{and} \quad \overset{e}{N}_2 = x/L \tag{19}$$

Element matrices for longitudinal motion can be determined using the trial functions:

Table 1: Element matrices and force vector of the longitudinal motion.

Stiffness Matrix (K)	Mass Matrixes (M)	Load vector (P)
$\overset{e}{A}\overset{e}{E}/\overset{e}{L}\begin{bmatrix}1&0&-1&0\\0&0&0&0\\-1&0&1&0\\0&0&0&0\end{bmatrix}\begin{matrix}q_1\\q_2\\q_7\\q_8\end{matrix} + \overset{e}{A}\overset{e}{G}/\overset{e}{L}^2\begin{bmatrix}0&0&0&0\\0&-q_2&0&q_8\\0&0&0&0\\0&q_2&0&q_8\end{bmatrix}\begin{matrix}q_1\\q_2\\q_7\\q_8\end{matrix}$	$\overset{e}{\rho}\overset{e}{A}\overset{e}{L}\begin{bmatrix}1/3&0&1/6&0\\0&0&0&0\\1/6&0&1/3&0\\0&0&0&0\end{bmatrix}\begin{matrix}\ddot{q}_1\\\ddot{q}_2\\\ddot{q}_7\\\ddot{q}_8\end{matrix}$	$\left\{\overset{e}{P}_x\right\}^T = \left\{\frac{\overset{e}{f}_a}{2L} + F_1 \quad -\frac{V_{oy1}^2}{AG} \quad \frac{\overset{e}{f}_a}{2L} - F_2 \quad \frac{V_{oy2}^2}{AG}\right\}$

Similarly, applying the motion in transverse planes directions x-y, x-z. In the most practical application requires any two of the following four:

- Essential BC's: $v = v_o$, $\dfrac{\partial v}{\partial x} = \phi_{oz}$
- Natural BC's: $E\,I\dfrac{\partial^2 v}{\partial x^2} = M$, $\overset{e}{E}\overset{e}{I}\dfrac{\partial^3 \overset{e}{v}}{\partial x^3} = V_o$

Similarly, applying the motion in torsional motion, in the most practical application requires the two possible boundary conditions for the torsional motion which are:

- Essential BC's: $\theta_x = \theta_{xo}$
- Natural BC's: $GJ\dfrac{\partial \theta_x}{\partial x} = T$

The local matrices and vectors in the transverse x-y and x-z and in torsional plane can be derived in the form:

Table 2: Element matrices and force vectors of the torsional and transverse motion.

Motion	Stiffness Matrixes K	Mass Matrixes M	Vector P
Torsional	$\dfrac{\overset{e}{G}\overset{e}{J}}{L}\begin{bmatrix} 1 & -1 \\ -1 & 1 \end{bmatrix}\begin{matrix} q_4 \\ q_{10} \end{matrix}$	$\overset{e}{\rho}\overset{e}{A}L\begin{bmatrix} \dfrac{\overset{e}{J}}{3\overset{e}{A}} & \dfrac{\overset{e}{J}}{6\overset{e}{A}} \\ \dfrac{\overset{e}{J}}{6\overset{e}{A}} & \dfrac{\overset{e}{J}}{3\overset{e}{A}} \end{bmatrix}$	$\begin{Bmatrix} \dfrac{\overset{e}{f_r}}{2L}+\overset{e}{T_1} \\ \dfrac{\overset{e}{f_r}}{2L}-\overset{e}{T_2} \end{Bmatrix}$
Transverse X-Y	$\overset{e}{E}\overset{e}{I_{zz}}/\overset{e}{L^3}\begin{bmatrix} 12 & 6\overset{e}{L} & -12 & 6\overset{e}{L} \\ 6\overset{e}{L} & 4\overset{e}{L^2} & -6\overset{e}{L} & 2\overset{e}{L^2} \\ -12 & -6\overset{e}{L} & 12 & -6\overset{e}{L} \\ 6\overset{e}{L} & 2\overset{e}{L^2} & -6L & 4\overset{e}{L^2} \end{bmatrix}+$ $\overset{e}{A}\overset{e}{E}(q_7-q_1)\begin{bmatrix} 6/5/\overset{e}{L^2} & 1/10/\overset{e}{L} & -6/5/\overset{e}{L^2} & 1/10/\overset{e}{L} \\ 1/10/\overset{e}{L} & 2/15 & -1/10/\overset{e}{L} & -1/30 \\ -6/5/\overset{e}{L^2} & -1/10/\overset{e}{L} & 6/5/\overset{e}{L^2} & -1/10/\overset{e}{L} \\ 1/10/\overset{e}{L} & -1/30 & -1/10/\overset{e}{L} & 2/15 \end{bmatrix}$	$\overset{e}{\rho}\overset{e}{A}\overset{e}{L}\begin{bmatrix} 13/35 & 11/210\overset{e}{L} & 9/70 & -13/420\overset{e}{L} \\ 11/210\overset{e}{L} & 1/105\overset{e}{L^2} & -13/420\overset{e}{L} & -1/140\overset{e}{L^2} \\ 9/70 & -13/420\overset{e}{L} & 13/35 & -11/210\overset{e}{L} \\ -13/420\overset{e}{L} & -1/140\overset{e}{L^2} & -11/210\overset{e}{L} & 1/105\overset{e}{L^2} \end{bmatrix}$ $+\overset{e}{\rho}\overset{e}{I}\begin{bmatrix} 6/5/\overset{e}{L} & 1/10 & -6/5/\overset{e}{L} & 1/10 \\ 1/10 & 2/15\overset{e}{L} & -1/10 & -1/30\overset{e}{L} \\ -6/5/\overset{e}{L} & -1/10 & 6/5/\overset{e}{L} & -1/10 \\ 1/10 & -1/30\overset{e}{L} & -1/10 & 2/15\overset{e}{L} \end{bmatrix}$	$\begin{Bmatrix} \dfrac{f_y L}{2}+V_{o1} \\ \dfrac{f_y L^2}{12}-M_{z1} \\ \dfrac{f_y L}{2}-V_{o2} \\ \dfrac{f_y L^2}{12}+M_{z2} \end{Bmatrix}$
Transverse X-Z	$\overset{e}{E}\overset{e}{I_{yy}}/\overset{e}{L^3}\begin{bmatrix} 12 & -6\overset{e}{L} & -12 & -6\overset{e}{L} \\ -6\overset{e}{L} & 4\overset{e}{L^2} & 6\overset{e}{L} & 2\overset{e}{L^2} \\ -12 & -6\overset{e}{L} & 12 & 6\overset{e}{L} \\ -6\overset{e}{L} & 2\overset{e}{L^2} & 6L & 4\overset{e}{L^2} \end{bmatrix}$ $+\overset{e}{A}E(q_7-q_1)\begin{bmatrix} 6/5/\overset{e}{L^2} & -1/10/L^e & -6/5/\overset{e}{L^2} & -1/10/L^e \\ -1/10/L^e & 2/15 & 1/10/L^e & -1/30 \\ -6/5/\overset{e}{L^2} & 1/10/L^e & 6/5/\overset{e}{L^2} & 1/10/L^e \\ -1/10/L^e & -1/30 & 1/10/L^e & 2/15 \end{bmatrix}$	$\overset{e}{\rho}\overset{e}{A}\overset{e}{L}\begin{bmatrix} 13/35 & -11/210\overset{e}{L} & 9/70 & 13/420\overset{e}{L} \\ -11/210\overset{e}{L} & 1/105\overset{e}{L^2} & -13/420\overset{e}{L} & -1/140\overset{e}{L^2} \\ 9/70 & -13/420\overset{e}{L} & 13/35 & 11/210\overset{e}{L} \\ 13/420\overset{e}{L} & -1/140\overset{e}{L^2} & 11/210\overset{e}{L} & 1/105\overset{e}{L^2} \end{bmatrix}$ $+\overset{e}{\rho}\overset{e}{I}\begin{bmatrix} 6/5/\overset{e}{L} & -1/10 & -6/5/\overset{e}{L} & -1/10 \\ -1/10 & 2/15\overset{e}{L} & 1/10 & -1/30\overset{e}{L} \\ -6/5/\overset{e}{L} & 1/10 & 6/5/\overset{e}{L} & 1/10 \\ -1/10 & -1/30\overset{e}{L} & 1/10 & 2/15\overset{e}{L} \end{bmatrix}$	$\begin{Bmatrix} \dfrac{f_{tz}L}{2}+V_{o1} \\ \dfrac{f_{tz}L^2}{12}-M_{y1} \\ \dfrac{f_{tz}L}{2}-V_{o2} \\ \dfrac{f_{tz}L^2}{12}+M_{y2} \end{Bmatrix}$

STRUCTURAL MATRICES

The procedure of assembling the stiffness, inertia matrices and load vectors is based on the requirement of "compatibility" at the element nodes. This means that at the nodes where elements are connected, the value of the unknown nodal degree of freedom or variable is the same for all the elements joining at that node [6,7].

Figure (7) illustrates the assembly of two one-dimensional elements. Each element has twelve degrees of freedom. The stiffness and Inertia matrices derived for different sets of independent displacements and accelerations can now be compiled to obtain the overall matrices of beam elements.

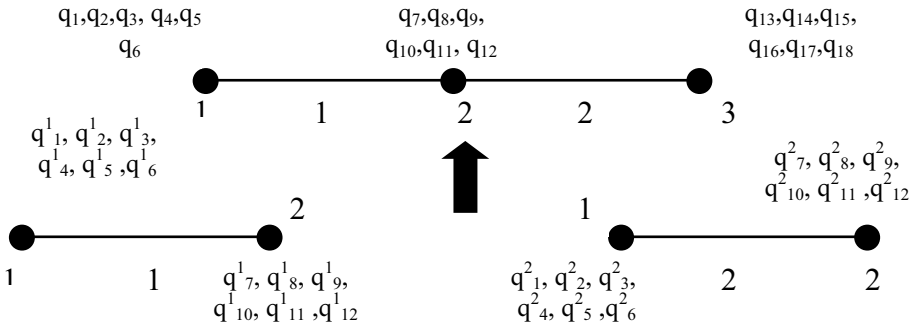

Figure 7: Assembly of two one–dimensional elements.

The general matrix equation of motion for nonlinearly undamped of the proposed model was expressed the following expression:

$$[M]\{\ddot{q}\}+[K]\{q\}=\{F\} \tag{20}$$

NUMERICAL SOLVER

This system of equations can be classified as a system of coupled ordinary differential equations of second order with the following characteristics:

- The order of the system matrices depending on the degrees freedom of each elastic element considered and number of the elastic elements considered.
- The Initial matrix is not a diagonal matrix.
- The stiffness matrix is not a diagonal matrix.
- Effect of load vector nonlinearity on the system is very small.
- The system is considered as a boundary value problem.

In order to solve such system of equations, a numerical approach was recommended over analytical methods. As the solution of the system of equations analytically is cumbersome and limited to a certain special forms, numerical methods have enough flexibility to solve non standard system of equations. Direct integration method was used to solve the equations of motion. In direct integration methods the system of equations are integrated using step by-step numerical integration procedure [6]. The use of direct integration methods eliminates the approximation caused by the transformation process from the finite element coordinates to eigen-coordinates and vise versa.

DISCUSSION OF THE RESULTS

In order to achieve this aim, three models differ in the number of nodes and the number of elements was chosen. Figure (8) represents model (1) of the three models chosen. Model (1): NE=4: DOF=21, model (2): NE=8: DOF=25 and model (3): NE=10: DOF=47. Three different types of cams motion were applied to cam mechanism in each model. A parabolic, simple harmonic and cycloidal were considered as the input signals to the system. The results of the flexible undamped three models running at speed of 3000 rpm were compared with results of the same rigid system responses of [9].

Figures (8), (10), and (11) represent the three models; (1), (2) and (3) flexible cam mechanisms. Figure 9 represents the external contact force between the cam surface and the face of the follower. The following assumptions were assumed in determination of

the force analysis of the selected models, the following assumptions were assumed:

- Bearings frictions were neglected.
- The effects of bearing clearance were neglected.
- Constant shaft speed.
- Constant shaft torque.
- Continuous contact between the follower and cam surface.

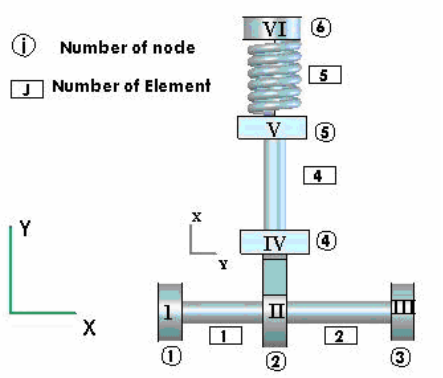

Figure 8: Model (1) of Cam mechanism.

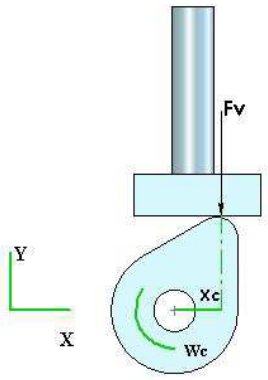

Figure 9: External force loads.

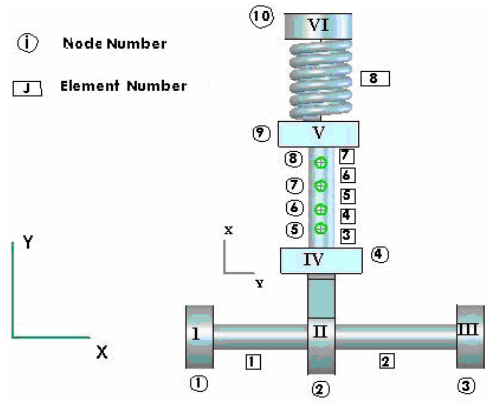

Figure 10: model (2) of Cam Mechanism.

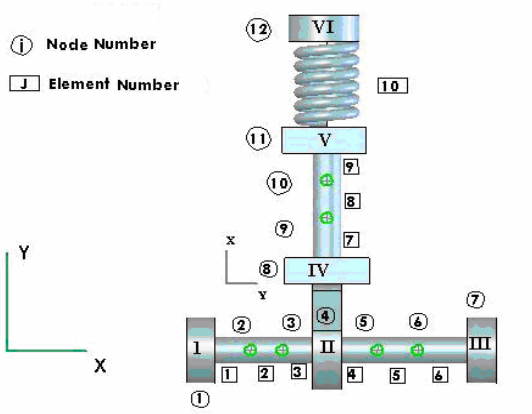

Figure 11: model (3) of Cam Mechanism.

In these models, it was considered that the retaining spring has an initial compressive force. The compressive force is equal to 2.5 times this force as calculated form rigid body conditions [4]. Such value of the retaining spring force was taken greater than 1 to insure continuous contact between the tappet and cam surface. It should be noted that the total force vector consists of two portions. The first part, is the initial compression in the retaining spring, while the second part, is a variable part depends on the elastic deformations of both camshaft and follower train. The contact force can be calculated by the following expressions:

$$P_V = P_{pr} + K_{KE}(Y_c + U_c) \tag{21}$$

$$K_{KE} = \frac{AE/L + K_{rs}}{AE/L \times K_{rs}} \tag{22}$$

$$P_{pr} = K_{KE} \times X_{rs} \tag{23}$$

The twisting torque was caused by the contact force and was calculated as follows:

$$T_{CF} = F_V X_C \tag{24}$$

$$X_C = \frac{V_F}{\omega_C} \tag{25}$$

For example, the general load vector of the flexible model (1) was expressed by the following expression:

$$p = \{0 \quad 0 \quad 0 \quad 0 \quad 0 \quad 0 \quad 0 \quad -p_v \quad 0 \quad -T_{CF} \quad 0 \quad 0 \quad 0 \quad 0 \quad 0 \quad 0 \quad 0 \quad 0 \quad p_v \quad 0 \quad 0\}^T \tag{26}$$

This approach was applied to all models.

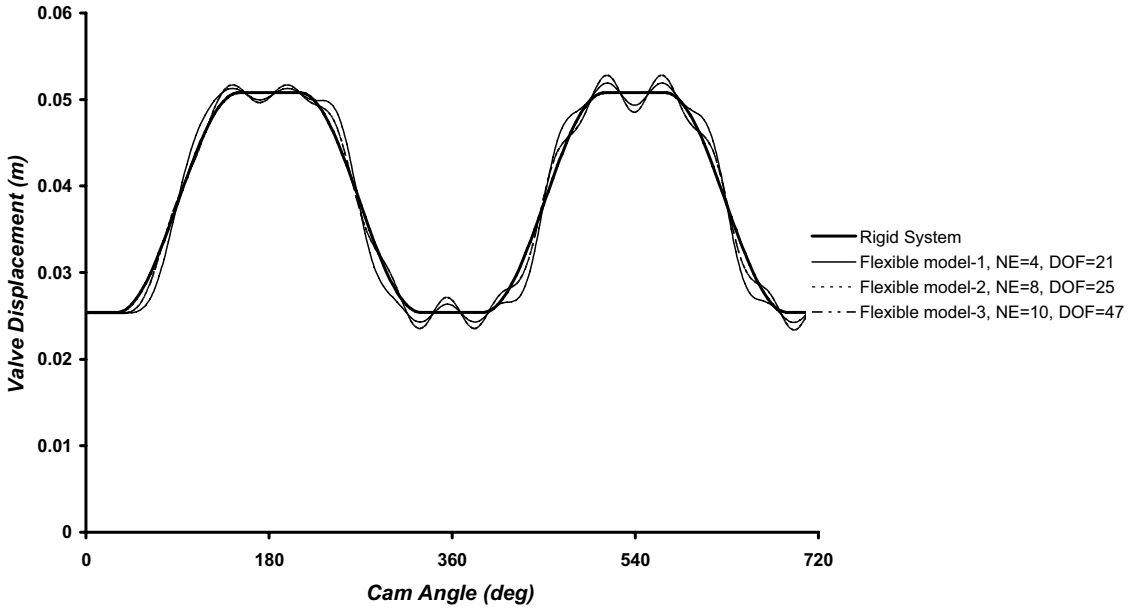

Figure 12: Displacement of valve for undamped system, S.H.M, n=3000 rpm.

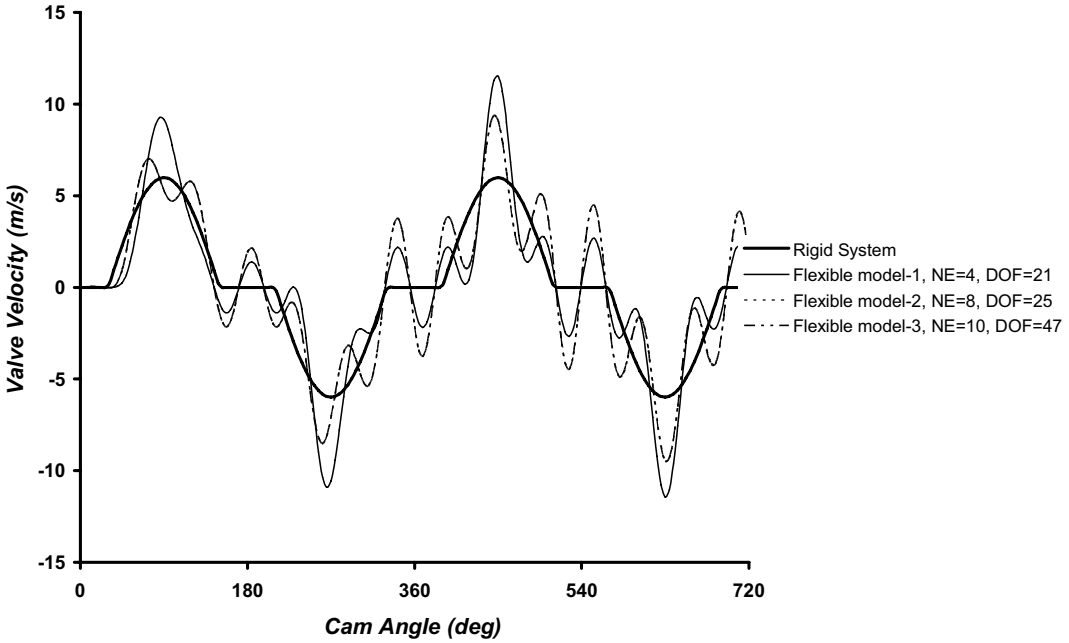

Figure 13: Velocity of valve for undamped system, S.H.M, n=3000 rpm.

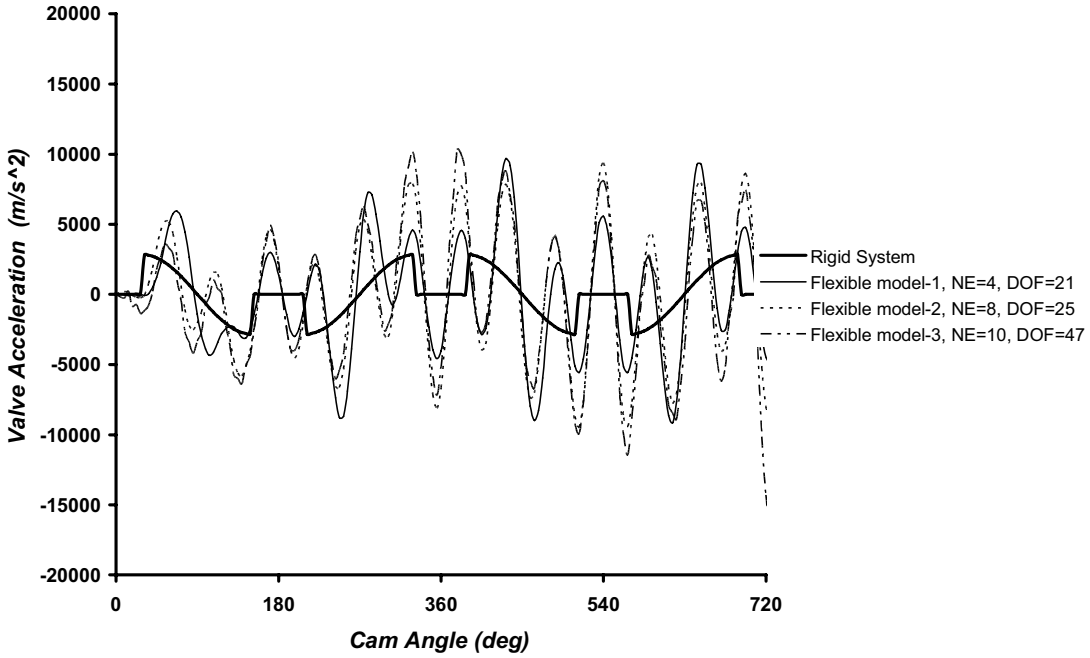

Figure 14: Acceleration of valve for undamped system, S.H.M, n = 3000 rpm.

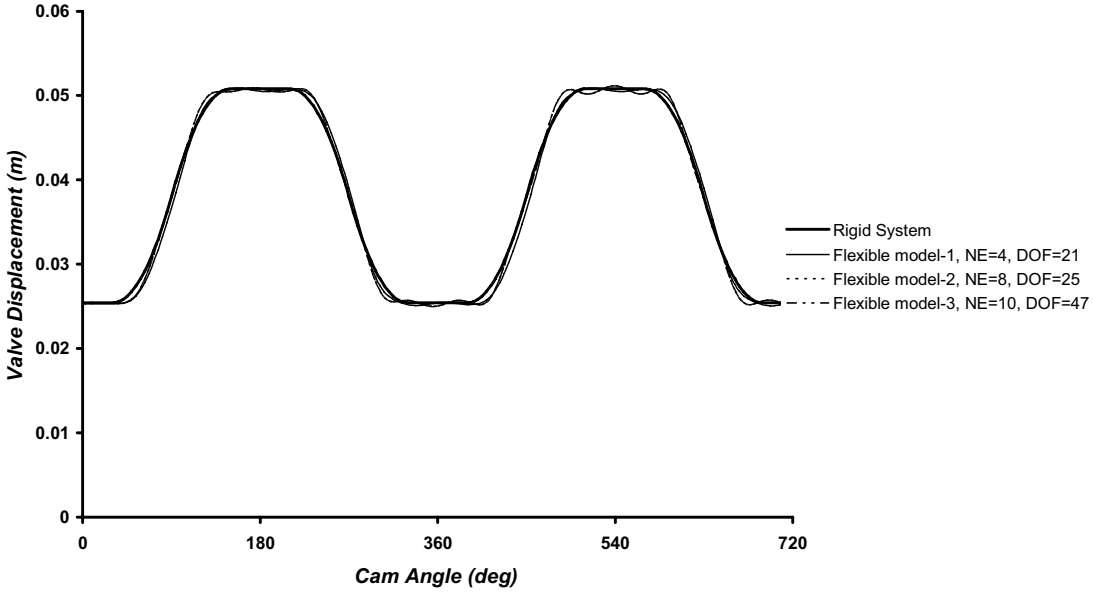

Figure 15: Displacement of valve for undamped system, Parabolic Motion, n = 3000 rpm.

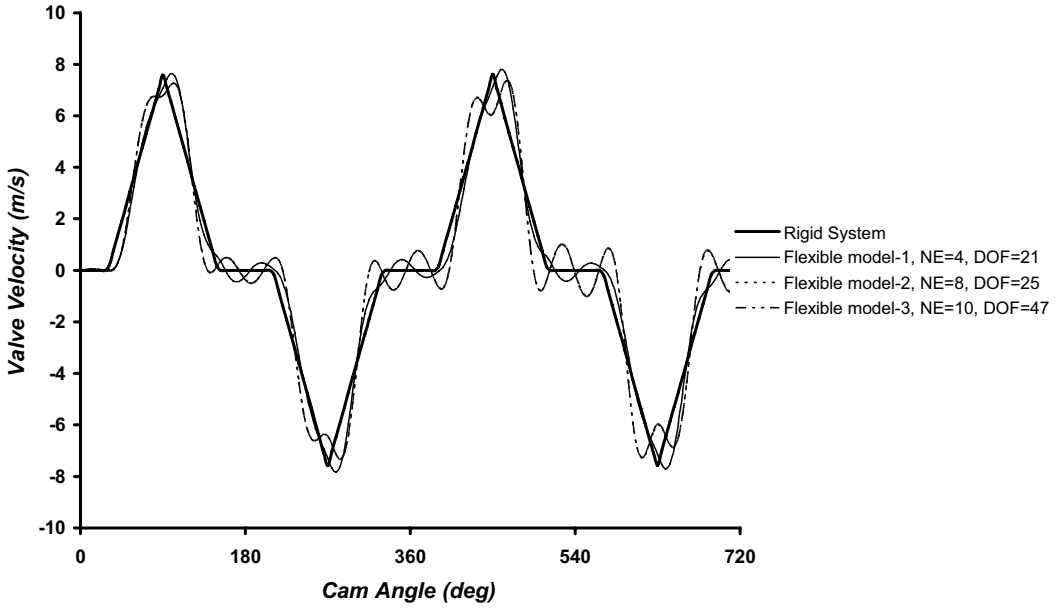

Figure 16: Velocity of valve for undamped system, Parabolic Motion, n = 3000 rpm.

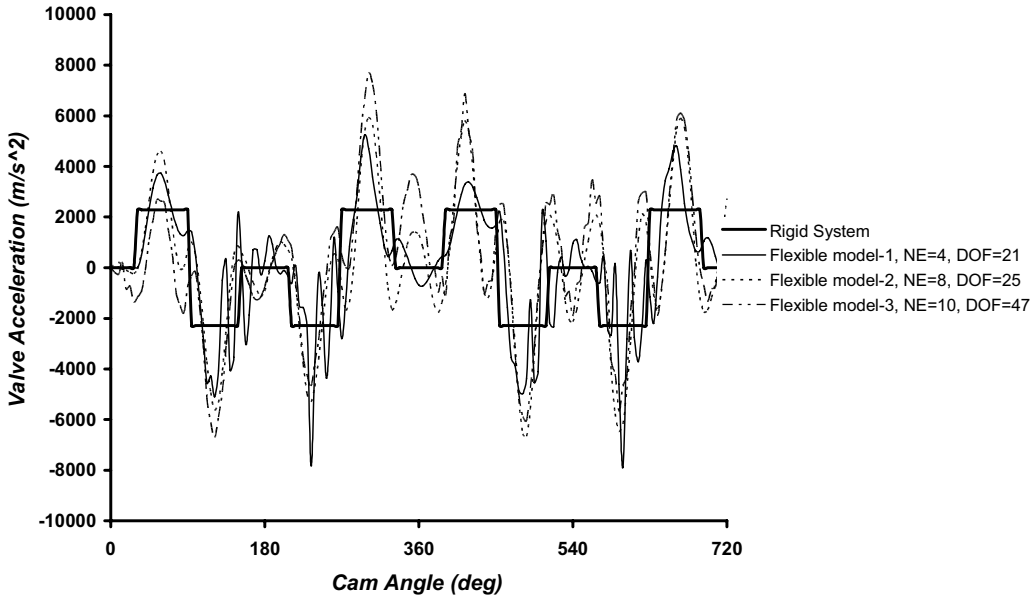

Figure 17: Acceleration of valve for undamped system, Parabolic Motion, n = 3000 rpm.

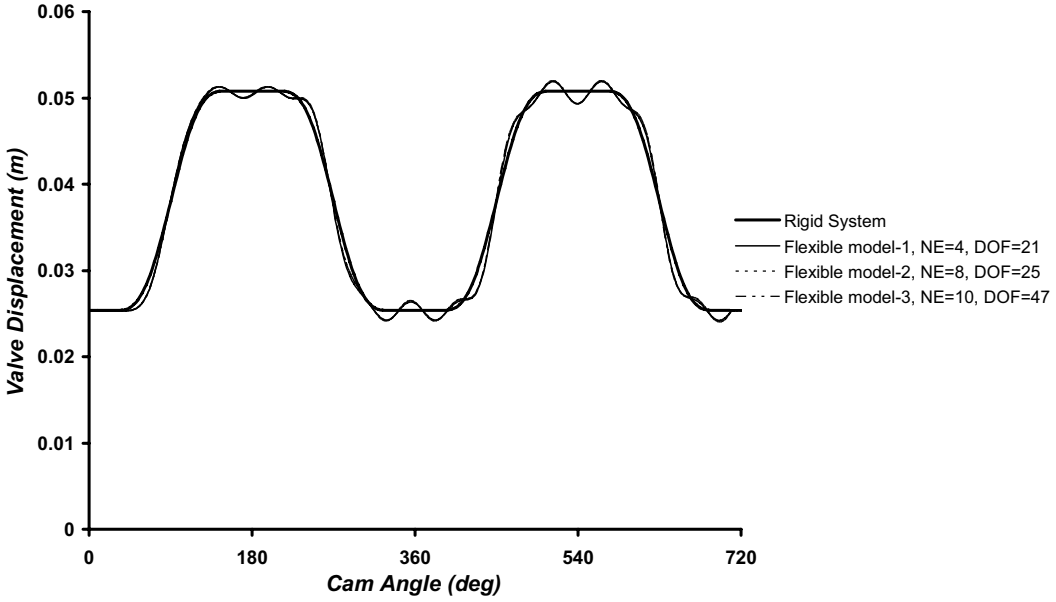

Figure 18: Displacement of valve for undamped system, Cycloidal Motion, n = 3000 rpm.

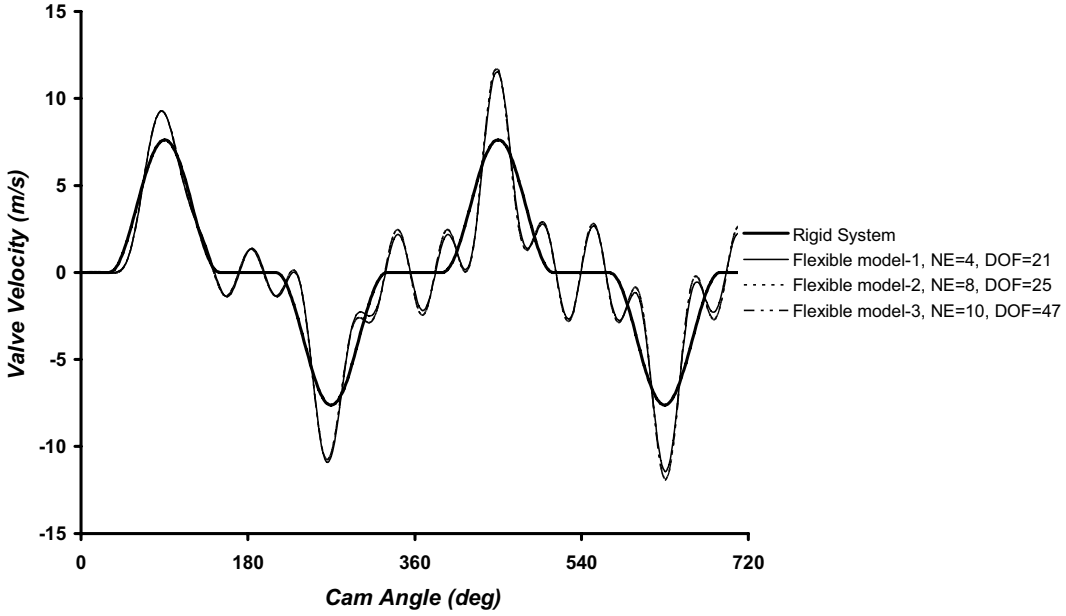

Figure 19: Velocity of valve for undamped system, Cycloidal Motion, n = 3000 rpm.

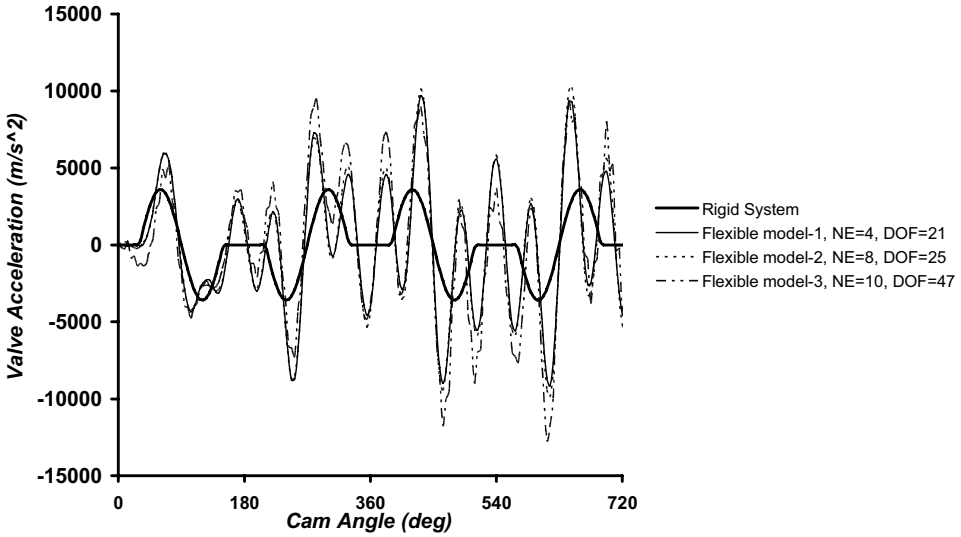

Figure 20: Acceleration of valve for undamped system, Cycloidal Motion, n = 3000 rpm.

The valve displacements are shown in Figure (12), Figure (15), and Figure (18) for simple harmonic, parabolic and cycloidal undamped systems respectively. Higher displacement and velocity responses of the S.H.M. motion occurred, whereas higher acceleration responses of the cycloidal motion occurred. It can be seen that, in all three models, for the three signal motions, the acceleration responses were deviated more from the rigid system than the other motions.

The results show that the system vibrations differ according to two factors; Firstly, in the flexible system, the response of model (1) shows less flexibility effects than model (3). Secondly, the response of parabolic shape shows less vibrational effects as stated by [8,9]. These effects can be referred to the discontinuity of the jerk curve for both parabolic and S.H.M cams [9]. As mentioned before, the response amplitudes depend on the flexibility of the system and the cam motion [9]. Figures (13), (16), and (19), represent the velocity of undamped systems while Figures (14), (17) and (20) show the acceleration for the undamped system, for the simple harmonic, parabolic, and cycloidal cam motion respectively.

It was noted that whenever the elasticity in the system was considered, a complete response analysis can be evaluated at any point of interest in the system.

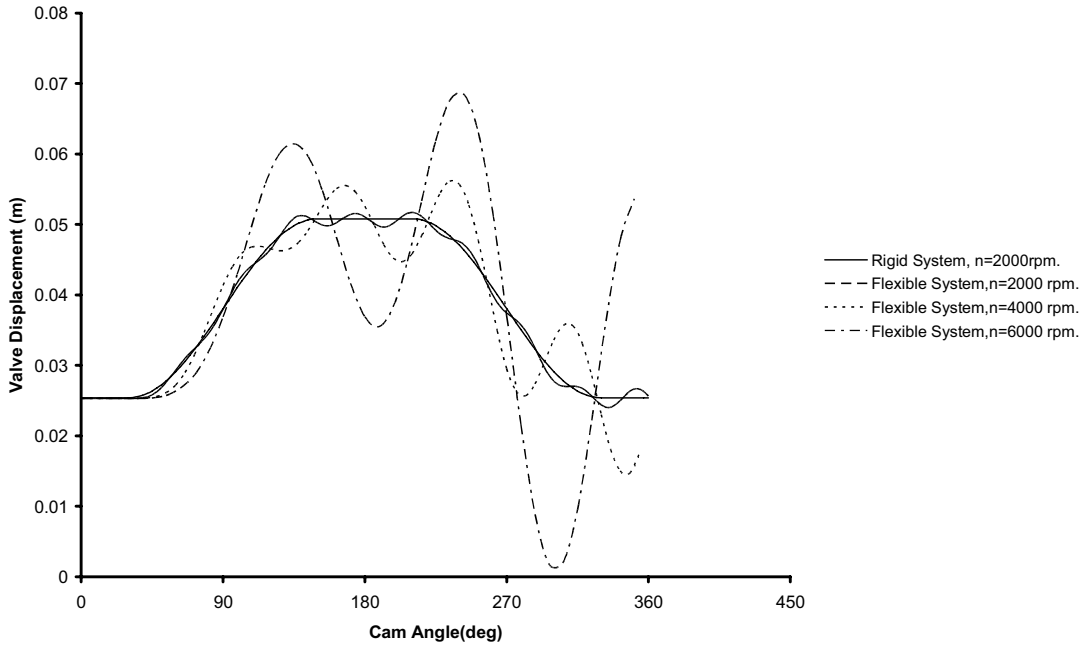

Figure 21: Valve displacement of model (1): S.M.H , undamped system at different speeds.

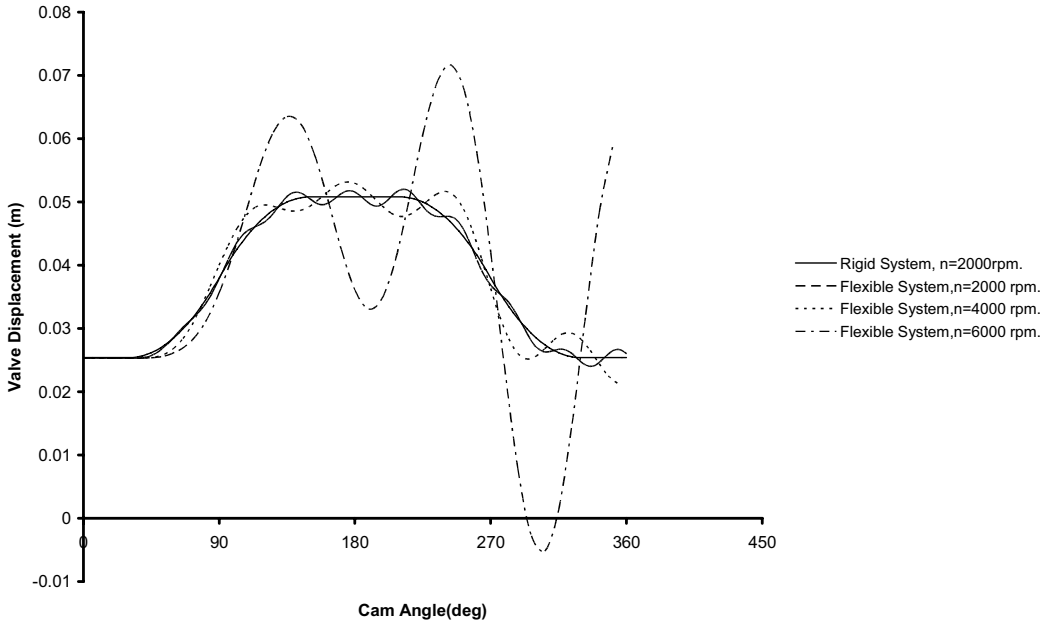

Figure 22: Valve displacement of model (1): Parabolic, undamped system at different speeds.

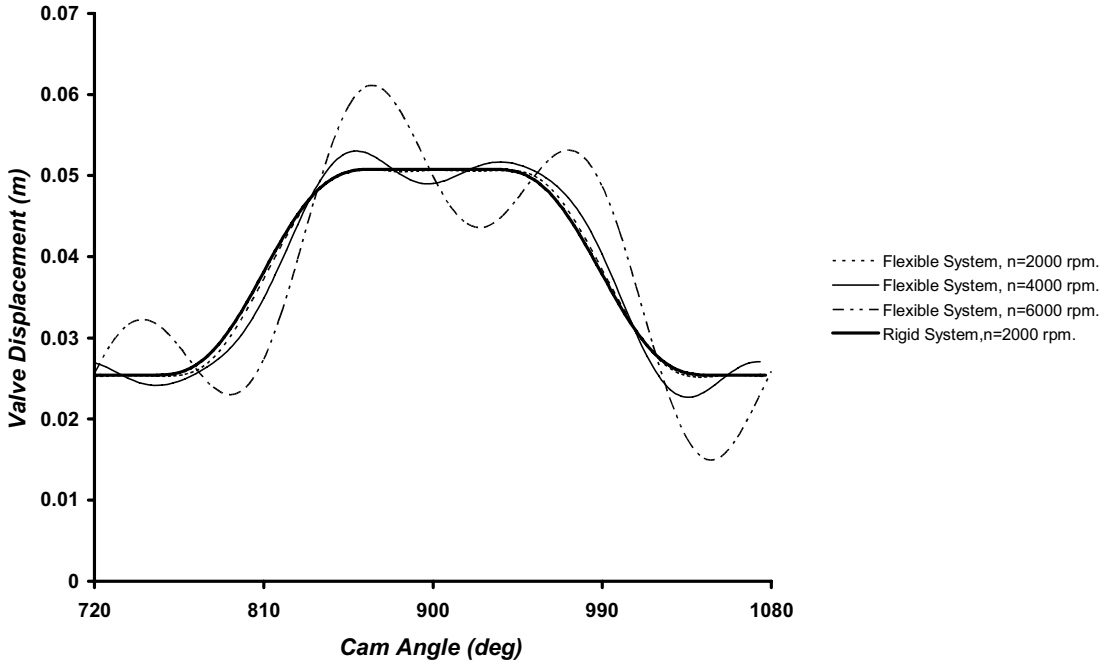

Figure 23: Valve displacement of model (1): Cycloidal, undamped system at different speeds.

The effect of input speed on the valve response for different cam motion can be seen in Figures (21), (22) and (23). These figures represent the valve response of the model (1) system for the S.H.M, parabolic and cycloidal cam motions running at

different input speeds. It is clear that as the speed increases the tendency to increase of vibration amplitude also increases. This is very clear for S.H.M and parabolic motions Figure (21) and Figure (22) which become unstable at speed of 4000 rpm. It is clear from all of these figures that the results obtained from the model (1) running at speeds 2000 rpm and less are very close to the results obtained from rigid body system. All figures show higher deviations than the rigid system of S.H.M input signals at cam angles 180, 360^o, 540^o and 720^o. This means that higher flexibility exists whenever the valve is completely closed or wide open. This leads to low cam performance.

CONCLUSIONS

A flexible cam mechanism was investigated by considering the flexibility of both cam shaft and cam follower train. A formulation of system of equations based on finite element technique was presented. A numerical technique was used to solve these differential equations. The system responses were obtained. Comparison of the obtained results with results obtained from previous work of rigid system [9] was presented. It can be concluded that higher displacement and velocity responses of the S.H.M. motion occurred, whereas higher acceleration responses of the cycloidal motion occurred. It also can be concluded that the flexible system response deviation from rigid system response and sensitive to number of DOF of the model. In general all the responses of all models show higher deviation from the rigid system at cam angle that produce wide open or complete closure of the valve. It is also highly recommended that investigations should be extended to cover the effect of elasticity friction and material damping of bearings on cam system responses.

REFERENCES

[1] Barkan, P., "Calculation of High –speed valve Motion with A flexible overhead Linkage", SAE. Trans. Vol. 61, 1953, pp. (687-700).

[2] Szakallas, L. E. and Savage, M., "The Characterization of Cam Drive System Windup", Trans. ASME, Journal of Mechanical Design. Vol. 120, April, 1980, pp.(278-285).

[3] Kim, W. J. and Newcombe, W. R., "The Effect of Cam Profile Errors and System Flexibility on Cam Mechanism Output" Mechanisms Machine Theory, Vol. 17, 1982, pp. 57-72

[4] Grewal, P. S., and Newcombe, W. R., "Dynamic Performance of High–speed Semi Rigid Follower Cam System, Effects of Cam Profile Errors", Mechanisms Machine Theory, vol. 23, No. 2, 1988, pp. (121-133).

[5] Al-Aribe, K. M., "Vibration Analysis of Flexible Cam Mechanisms", M. Sc. Thesis, 1999, Benghazi, Libya.

[6] Rao, S.S., "The Finite Element Methods in Engineering", Butterworth-Heinemann, Third Edition, 1999.

[7] Rothbart, H. A, "Cams. Design, Dynamics and Accuracy" J. Wiley, 1956.

[8] Pisano, A.P., and Freudenstein, F., "An Experimental and Analytical Investigation Of The Dynamic Response of a High-Speed Cam-Follower System", Part2: A Combined, Lumped /Distributed Parameter Dynamic Model", Trans ASME, Journal of Mechanism, Transmissions, and Automation in Design, Vol. 105, December, 1983, pp. (699-704).

[9] Chen, F. Y., "Mechanics and Design of Cam Mechanisms" Wiley, 1982.

NOMENCLATURE

u_o	*Initial displacement vector*
V_o	*shear force*
F_o	*Axial force*
$f_t(x,t)$	*Transverse distributed force*
v	*Transverse displacement*
ρ	*Density*
A	*Cross-sectional area*
I	*Cross-sectional area moment of inertia*
E	*Modulus of elasticity*
u	*Axial displacement*
$f_a(x,t)$	*axial Distributed force*
θ_x	*Angular displacement about x-axes*
T	*Torque force*
$f_r(x,t)$	*Torque Distributed force*
J	*Polar moment of inertia of the cross sectional area*
G	*Shear modulus of elasticity*
N	*Trail function*
NE	*Number of element*
L	*Length of element*
e	*Element number*
q	*Generalized degrees of freedom*
K_{rs}	*Retaining spring stiffness*
M_{rs}	*Mass of the retaining spring*
$M_{eq(rocker+valve\ Side)}$	*mass equivalent for valve side and rocker*
$M_{Valve\ Side}$	*all masses at side valve*
I_{rocker}	*moment of inertia for rocker about the rocker shaft*
K_{eq}	*equivalent spring stiffness at the cam side*
X_{rs}	*Initial compression of the retaining spring*
P_V	*Contact force between the cam surface and the face of the follower train*
P_{pr}	*Preload force (due to the initial compression of the retaining spring)*
K_{KE}	*Equivalent follower train stiffness*
Y_c	*Rigid cam lift*
U_c	*Cam shaft deflection at the cam*
T_{CF}	*Twisting torque to the cam shaft*
X_C	*Perpendicular distance form the applied force to the cam center,*
V_F	*contact point velocity*
ω_C	*Cam shaft angular velocity*